Original papers
Materials for energy and environment, next-generation photovoltaics, and green technologies

УДК 66.081.6 DOI: 10.17277/jamt.2021.01.pp.042-053

Studies of the pore space of the UPM-K, UAM-50, UAM-100 composite ultrafiltration membrane

Sergey I. Lazarev[a], Olga A. Kovaleva[a,b], Irina V. Khorokhorina[a], Tatyana A. Khromova[a]✉, Sergey V. Kovalev[a,b]

[a] *Tambov State Technical University, 106, Sovetskaya St., Tambov, 392000, Russian Federation,*
[b] *Derzhavin Tambov State University, 33, Internatsionalnaya St., Tambov, 392000, Russian Federation*

✉ tatyanka.xromova96@mail.ru

Abstract: The development of methods for assessing the distribution of pores by radii (or diameters) and studying the microstructure of the surface of a membrane partition is an urgent task. The authors of the paper carried out experimental studies of the pore diameter distribution for the UPM-K ultrafiltration membrane, determined the porosity and hydrodynamic permeability of the UAM-50, UAM-100 membranes. The analysis of the experimental results showed that the UPM-K ultrafiltration membrane had an average pore diameter of 54 nm. The UAM-50 and UAM-100 membranes were characterized by an asymmetric structure (an active layer (dense) and a porous substrate), while the pores were 2.5–40 and 10–40 nm in size, respectively. The experiments on the study of the hydrodynamic permeability of UAM-50, UAM-100 ultrafiltration membranes when separating a solution of sodium lauryl sulfate showed that the kinetic response curves of the "membrane-solution" system were conventionally divided into two stages. The first stage of the process was faster and lasted only a few minutes. After 7.8 and 13.05 min, the hydrodynamic permeability decreased by ~ 27 %, 7 %, which was due to structural changes in the cellulose acetate layer under the action of mechanical load (transmembrane pressure). The second stage was slower – with a duration of ~ 33 and 60 min and a decrease in hydrodynamic permeability by 41 % and 11 %. Based on the analysis of the approximating function, the rate constants of the membrane separation of solutions and the empirical coefficients of the equation are found.

Keywords: membrane pore space; pore diameter; normal distribution function; electron microscopic studies.

For citation: Lazarev SI, Kovaleva OA, Khorokhorina IV, Khromova TA, Kovalev SV. Studies of the pore space of the UPM-K, UAM-50, UAM-100 composite ultrafiltration membrane. *Journal of Advanced Materials and Technologies*. 2021;6(1):42-53. DOI: 10.17277/jamt.2021.01.pp.042-053

Исследования порового пространства композитной ультрафильтрационной мембраны УПМ-К, УАМ-50, УАМ-100

С. И. Лазарев[а], О. А. Ковалева[а,б], И. В. Хорохорина[а], Т. А. Хромова[а]✉, С. В. Ковалев[а,б]

[а] *Тамбовский государственный технический университет,*
ул. Советская, 106, Тамбов 392000, Российская Федерация,
[б] *Тамбовский государственный университет им. Г. Р. Державина,*
ул. Интернациональная, 33, Тамбов 392000, Российская Федерация

✉ tatyanka.xromova96@mail.ru

Аннотация: Разработка методик оценки распределения пор по радиусам (или диаметрам) и исследования микроструктуры поверхности мембранной перегородки является актуальной задачей. Авторами работы проведены экспериментальные исследования распределения пор по диаметрам для ультрафильтрационной мембраны УПМ-К, определены пористость и гидродинамическая проницаемость мембран УАМ-50, УАМ-100. Анализ результатов эксперимента показывает, что ультрафильтрационная мембрана УПМ-К имеет среднее значение диаметров пор – 54 нм. Для мембран УАМ-50, УАМ-100 характерна ассиметричная структура (активный слой (плотный) и пористая подложка), при этом поры имеют размеры 2,5…40,0 нм и 10…40 нм, соответственно. Эксперименты по исследованию гидродинамической проницаемости ультрафильтрационных мембран УАМ-50, УАМ-100 при разделении раствора лаурилсульфата натрия показали, что кинетические кривые отклика системы

«мембрана-раствор» условно разделяются на две стадии. Первая стадия процесса протекает быстрее и длится всего несколько минут. Через 7,80 и 13,05 мин гидродинамическая проницаемость уменьшается соответственно на ~ 27 и 7 %, что обусловлено структурными изменениями в ацетатцеллюлозном слое под действием механической нагрузки (трансмембранного давления). Вторая стадия более медленная – продолжительностью ~ 33 и 60 мин с уменьшением гидродинамической проницаемости соответственно на 41 и 11 %. На основе анализа аппроксимирующей функции найдены константы скорости мембранного разделения растворов и эмпирические коэффициенты уравнения.

Ключевые слова: поровое пространство мембраны; диаметр пор; функция нормального распределения; электронно-микроскопические исследования.

Для цитирования: Lazarev SI, Kovaleva OA, Khorokhorina IV, Khromova TA, Kovalev SV. Studies of the pore space of the UPM-K, UAM-50, UAM-100 composite ultrafiltration membrane. *Journal of Advanced Materials and Technologies*. 2021;6(1):42-53. DOI: 10.17277/jamt.2021.01.pp.042-053

1. Introduction

At industrial enterprises of the Russian Federation, CIS countries and foreign countries in various industries (petrochemistry, chemical engineering), baromembrane separation processes are used to regenerate different solutions. At the same time, there is a problem of ensuring high quality indicators for the purification of various aqueous media containing both organic and inorganic compounds. The processes of membrane purification of various technological solutions, especially food and biological ones, are accompanied by sedimentation and fouling of the membrane surface. The study of various characteristics of membranes depends on many factors (differential transmembrane pressure, electric potential on the membrane, etc.). In a particular case, similar characteristics are associated with the hydrodynamic permeability of the solution through the membrane, and this also depends on the distribution of pores along the radii for a particular type of membrane. The development of methods for assessing the distribution of pores by radii (or diameters) and the study of the surface microstructure for a particular membrane partition is still relevant today [1–11].

In [12], the information was presented on the development of a digital image processing software package for calculating porosity, pore diameter distribution, pore area distribution and pore shape distribution on the membrane surface by processing images of the membrane surface and cross section obtained using SEM. Comparison with the results of the analysis using the IBAS I/II image analysis instrument (made in Germany), the porosity analyzed by the developed software package is larger, while the distribution variance is wider.

The problems and prospects of using the ultrafiltration method in the separation of solutions and water purification were described in [13]. The pore size for ultrafiltration membranes ranged from 5 nm to (0.05–0.1) μm. The authors showed micrographs made using an electron microscope when studying polymer membranes made of various materials, for example, cellulose acetate, polyethersulfone, etc.

The authors of [14] proposed a new, simple and effective test for pore size based on the synthesis and transfer of hard nanoparticles across the membrane. Monodispersions of gold and silver 3–50 nm provided a complete pore size distribution, including d100, the pore diameter at which the membrane had 100 % retention capacity. The maximum pore size in the UV membrane structure was difficult to determine by other methods, although it was necessary for accurate separation analysis. The d100 values in the tested UV membranes ranged from 40 nm to 50 nm depending on the membrane material. Polymer membranes were more flexible than ceramic membranes and their d100 are usually much higher than MWCO.

Application of ultrafiltration solutions for purification processes is one of the most important stages in the production of high-purity water, liquid chemicals and biopharmaceutical products.

For example, in [15], the findings of the study of PA-100 ultrafiltration membranes based on aromatic polyamide performed on a SmartSPM-1000 atomic force microscope were described. The images obtained in this way passed the procedure for identifying pore sizes based on the Gwyddion program by two different methods (threshold and watershed). A statistical analysis procedure was carried out to study the pores. The authors noted that the watershed method allowed obtaining more detailed and reliable information on the distribution of the pores of the studied membrane over its surface.

Based on the analysis of the literature data and the demand for research on the identification of membrane pore sizes on the surfaces of ultrafiltration

membranes, we selected the objects for the research and the experimental procedure.

In the processes of membrane separation of solutions, the kinetics of the process is determined by the efficiency and productivity of purification and concentration of technological and industrial solutions. An important role in the study of the mechanism is given to the structural characteristics of membranes, which affect the kinetics of the membrane process. The authors in [16] analyzed the data on specific output flux and retention capacity for several commercial membranes, including the ESPA membrane, which shows good results in the separation of solutions containing NaCl, $(NH_4)_2CO_3$. It was found that the degree of separation is influenced by such factors as the molecular weight and molecular structure of the solute.

In [17], the authors investigated a low-pressure membrane process for removing cerium and neodymium from industrial solutions, where the permeability was analyzed by the concentration of the solute using inductively coupled plasma atomic emission spectroscopy.

The authors of [18] presented a classification of membranes and membrane water treatment methods according to various criteria, analyzed membrane separation methods and the possibility of their application for wastewater treatment of chemical and oil refineries. It was noted that hybrid technologies based on the use of membrane catalytic reactors with ultrafiltration ceramic or metal-ceramic membranes in the presence of ozone are the most preferable for the treatment of wastewater from chemical and petrochemical enterprises.

The authors of [19] calculated the hydrodynamic permeability of a membrane consisting of a set of porous spherical particles with a rigid impermeable core. The calculations used the cell method proposed by Happel and Brenner.

In [20], the authors investigated the ultrafiltration process using a polysulfone membrane. Membranes were prepared by phase inversion using a polysulfone (PSf) polymer base, polyvinylpyrrolidone (PVP), and N-methyl-2-pyrrolidone (NMP). The characteristics of the morphology of the surface layer were determined using SEM and atomic force microscopy (AFM).

In [21], the authors studied the mechanism of fouling of various types of UV membranes with different pore sizes by cross-flow filtration of biological suspensions. The experiments were carried out using two types of membranes (cellulose-oxy- and polyethersulfone) and three substances with different molecular weights.

In [22], the possibility of using electrosynthesized ultrafiltration membranes for concentration and purification from phenolic impurities of aqueous extracts of arabinogalactan was shown. It was found that the modification of the surface of ion-exchange membranes with ionic surfactants of various natures makes it possible to increase the separation of mono- and divalent ions by a factor of 2–3 in comparison with industrial ion-exchange membranes.

The issues of evaluating the resources of membrane performance are considered in the article [23], where the authors carry out a theoretical analysis of the operation of low-pressure membranes in the process of separation of solutions. In [24], the authors noted that the pore size of the membrane and surface porosity mainly regulate the morphology of the PSU membrane, which increases the efficiency of the membranes and reduces membrane fouling. In [25], the structure and permeable properties of the surface of the initial UV membranes made of polysulfone (PS-100), polyacrylonitrile (PAN-100) and modified by applying thin films of polyvinylpyridine by the Langmuir-Blodgett method were studied by atomic force microscopy. It has been established that the deposition of thin films on the PS-100 membrane leads to a twofold decrease in the specific output flow for water, but a significant increase in the retention coefficient is observed.

The analysis of the studies [1–25] made it possible to evaluate the significance of kinetic and structural characteristics in the processes of ultrafiltration separation of solutions containing surfactants.

Therefore, the aim of the paper is to conduct experimental studies of the pore diameter distribution for the UPM-K UV membrane and to determine the porosity and hydrodynamic permeability of the UAM-50, UAM-100 membranes.

2. Materials and methods

2.1. Materials

The object of the study was the UPM-K, UAM-50, UAM-100 UV membranes (ZAO STC Vladipor, Vladimir), the characteristics of which are presented in Table 1 [26].

The choice of porous ultrafiltration membranes as the object of the study is due to high retention capacity, good performance and its maximum applicability in industrial practice.

Table 1. Characteristics of the UPM-K, UAM-50, UAM-100 type membranes

Permeable membrane brand	Permeable membrane type	Active layer material	Specific solvent flow J, m^3/m^2 s, for P = 0.5 MPa	Retention rate for 0.15 % NaCl solution
UPM-K	Composite	Polyamide	$1.16 \cdot 10^{-5}$	0.980
UAM-50		Cellulose acetate	$2.00 \cdot 10^{-5}$	0.985
UAM-100			$1.00 \cdot 10^{-5}$	0.985

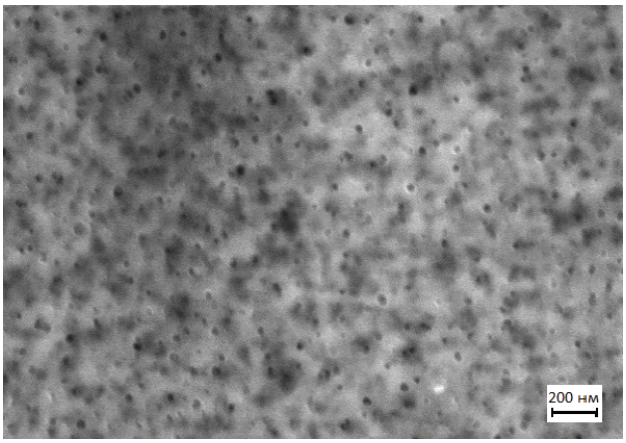

Fig. 1. Electronic image of a sample of the UPM-K ultrafiltration membrane at a magnification of 100 and an accelerating voltage of 5 kV

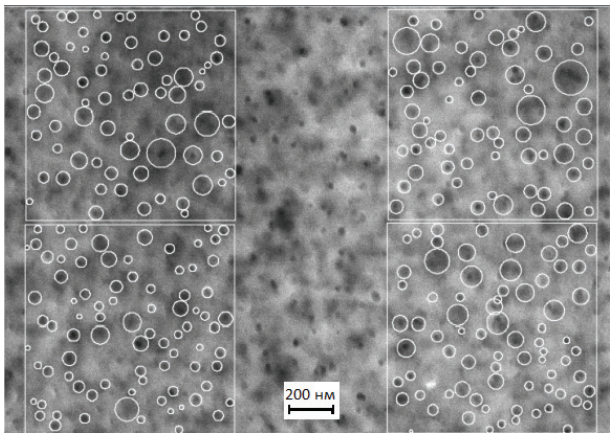

Fig. 2. Electronic image of the surface of the UPM-K ultrafiltration membrane with three uniform regiond along the perimeter at a magnification of 100 and an accelerating voltage of 5 kV

2.2. Methods

The surface of dry samples of UPM-K, UAM-50, UAM-100 ultrafiltration membranes was examined using a Merlin scanning electron microscope (CarlZeiss, Germany, Center for Collective Use of Research Equipment of Derzhavin Tambov State University) (Fig. 1). Some of the original images were transferred exactly to scale into the AutoCad 2018 CAD environment, where further image processing took place.

First, in the photographs of the membrane surface (Fig. 2), three uniform regions were visually selected (without significant deviations of the geometric elements of the surface microstructure). The area of the selected square elements was $1 \cdot 10^6$ nm^2, the scale of the regions strictly corresponded to the scale of the photographs. Then the pores were visually determined, which were described by a circle using the program. After marking the pores, the procedure for exporting data to the automated design system AutoCad 2018 was carried out using the console command EXTRACT DATA. Radial dimensions on the surface (active) layer of the membrane in nm were calculated using the AutoCad2018 program intended for computer-aided design.

Using the AutoCad 2018 software function of "data extraction", the main characteristics (diameter, area of each element) were found for all four square sample areas. Using the data retrieval function made it possible to perform surface analysis on each membrane.

To assess the error in determining the pore size, 5 electronic images were analyzed, obtained for different areas of the surface of the membrane under study. The procedure for processing each electronic image was repeated 10 times. The statistical processing of the results confirmed that the relative standard deviation did not exceed 0.1.

To calculate the area of the clean surface of the square sample areas, the sample areas were added, and then they were subtracted from the total sample area. Then the coefficient of contamination was determined according to the following calculation formula (1):

$$K = \frac{S_c}{S_d}, \quad (1)$$

where S_c, S_d are the area of the clean and darkened surface on the membrane, nm^2.

The obtained characteristics are presented in Table 2.

Table 2. Estimated area of the UPM-K membrane

Membrane type	Darkened surface area, S_d, m^2	Clean surface area, S_c, nm^2	Clogging coefficient, K
UPM-K	$793.1 \cdot 10^3$	$3.20 \cdot 10^6$	0.25

For analytical processing of the data obtained as a result of the research, Microsoft Excel 2010 was used. Using the descriptive statistics function, the program determined such parameters as the standard deviation and the average pore diameter.

For further calculations, it is necessary to verify the correctness of the analysis of the data obtained. This can be solved by constructing histograms. The construction of histograms is performed using the standard settings of Microsoft Excel 2010. The program performs an automated selection of the range obtained during the calculation of the data and builds histograms for the UPM-K membrane.

In the automated calculation of the computer, the range is independently selected, which is determined by the calculation formula (2):

$$R = X_{\max} - X_{\min}, \quad (2)$$

where $X_{\max}$ is maximum sample value; $X_{\min}$ is minimum sample value.

This parameter (range) shows what the width of the histogram will be and determines the spread of the obtained values. Then the computer divides the resulting range into several intervals, the number of which is calculated by the formula (3):

$$k = \sqrt{n \pm 2}, \quad (3)$$

where n is coefficient that takes into account the number of found sample diameters.

Then, by means of the computer, the width of the interval (h) was calculated by the formula (4):

$$h = \frac{R}{k}. \quad (4)$$

Then, the function of the normal distribution of the diameters of the pores of the membranes was constructed.

3. Results and discussion

3.1 Pore diameter distribution for UPM-K UV membrane

The standard deviation and the average pore diameter of the UPM-K ultrafiltration membrane determined on the basis of the study and the data obtained according to the previously presented method are presented in Table 3.

Fig. 3 shows a histogram of distribution of pore diameter sizes per intervals of pore diameter sizes for the UPM-K membrane.

The resulting histogram shown in Fig. 3 represent combs (multimodal type). Among the various laws, the most used is the normal distribution law (Gauss's law). According to Gauss's law, to which random variables obey, and they are significantly influenced by numerous, approximately equal in strength, factors. The results of multiple measurements obey this law, which is observed in our case [17]. Table 4 shows the values of the studied parameters.

Table 3. Average pore diameter and average deviation

Membrane type	Average pore diameter of d_{av}, nm	Standard deviation σ
UPM-K	54	1.21

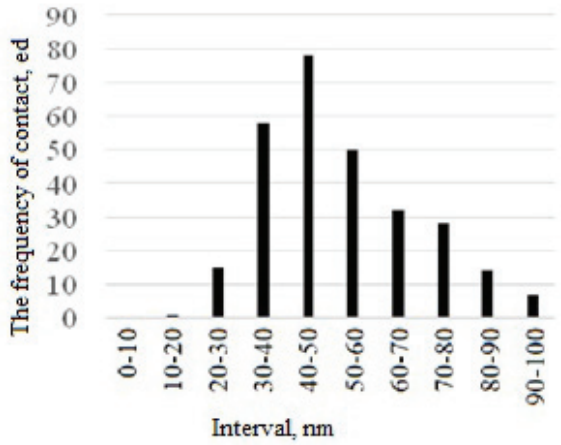

Fig. 3. Distribution of pore diameter sizes by pore diameter size intervals for the UPM-K membrane

Table 4. The main parameters

Membrane type	UPM-K
Standard deviation	20.6
Sample variance	423.6
Excess	1.5
Asymmetry	14.3
Interval	165.6

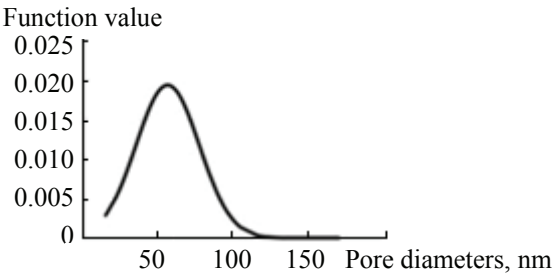

Fig. 4. Sample variance function of the UPM-K membrane from the distribution of the membrane pore diameters

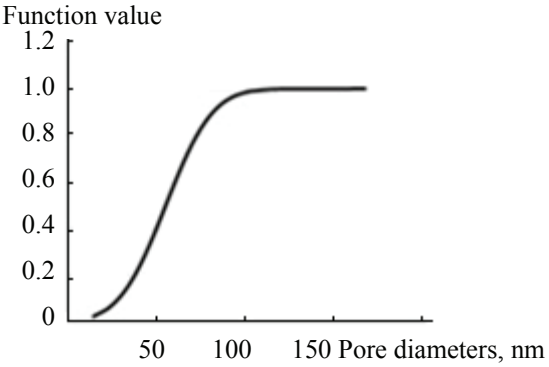

Fig. 5. The function of the normal (integral) distribution of the UPM-K membrane from the distribution of the membrane pore diameters

For the UPM-K membrane (Fig. 4, 5), the graph of the normal distribution function of pore diameters on the membrane is as follows.

According to the hypothesis about the correspondence of the empirical distribution to the normal law, it is necessary to study the reproducibility of the procedure, i.e. the possibility of studying the primary parameters of the process is determined: the arithmetic mean value and the standard deviation.

In analytical form, the normal distribution function for the UPM-K membrane, the following formula is proposed:

$$y = \frac{1}{54.54\sqrt{2\pi}} e^{\frac{(x-20)^2}{2\cdot 54.54^2}}. \quad (5)$$

Thus, we can claim that the UPM-K UV membrane has different pore diameters – the average hit range is 40–60 nm. It can be concluded that the size of the pores and their frequency of penetration per 1 mm^2 affects the permeable properties of the studied semi-permeable membranes and, most likely, affects the effect of their overgrowing.

3.2. Experimental studies of porosity of UAM-50, UAM-100 membranes

Membranes used in chemical technology for the separation of solutions and industrial effluents, carried out under the influence of transmembrane pressure (microfiltration, ultrafiltration, nanofiltration and reverse osmosis) or electric potential, are composite materials consisting of two (or even three) layers of different materials [28–30]. Resistance is usually an intrinsic property of the membrane, reflecting the pore structure. Due to the compositional structure of membranes, geometric or structural parameters cannot be determined by standard measurements, so other types of experiments are conducted to evaluate the thickness and / or porosity of each layer. Structural parameters are very important to predict the behavior of the membrane, since the permeable and selective properties of the membrane strongly depend on the structure of the pores and their distribution [28], which is also noted by the authors of [28–31]. In particular, ultrafiltation membranes are usually made as two series-connected homogeneous elements with different structural and transport properties [28–31]: a thin and dense active layer, a thick and porous substrate (Figs. 6, 7). Characterization of both layers provides the necessary information about the selectivity and performance of composite membranes.

The analysis of Figs. 6, 7 (*c*) electron images of UAM-50 and UAM-100 ultrafiltation membranes showed that the membrane actually consists of an active layer and a porous substrate. It is noted that the active layer of the UAM-50 membrane has a min thickness of up to 27 nm, and that of for UAM-100 has a min thickness of up to 15 nm.

On the surface of the UAM-50 and UAM-100 membranes, pores are visible, the average size of the diameter of which for several samples is 2.5÷40 nm and 10÷40 nm, respectively. Selected areas of the image are given for comparison and assessment, since along with small, medium pores, there are also wider ones, the size of which reaches 100 nm.

Analyzing the surface of the cross-section of membrane samples, two layers are observed: dense and more porous. The pore space is formed by through and dead-end bottle-shaped pores with diameters up to 40 nm, which are inhomogeneous along the entire pore length.

Also, when analyzing images, it can be concluded that the active layer of ultrafiltration membranes has an asymmetric pore structure. The active layer of the membrane can be divided into two components: a selective layer with a small pore size, and a pore substrate, in which the pores increase

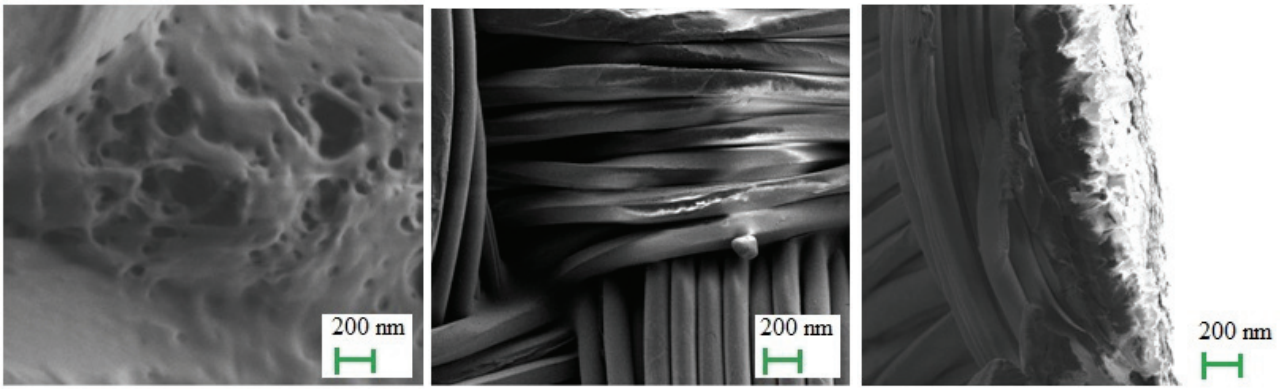

(*a*) (*b*) (*c*)

Fig. 6. Electronic images of the UAM-50 ultrafiltration membrane:
a – image of the membrane surface – its active layer; *b* – the substrate surface, for this membrane – fabric-type nylon;
c – image of an active cellulose acetate layer section of a substrate membrane

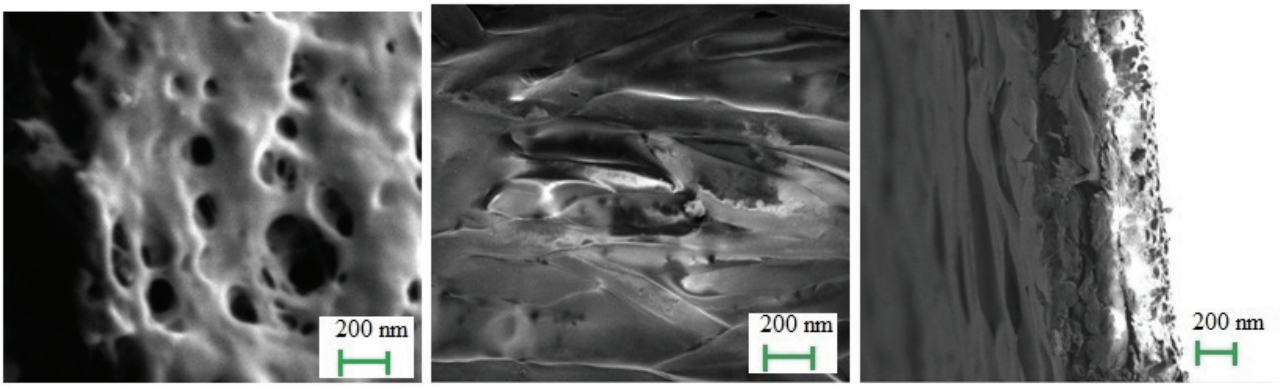

(*a*) (*b*) (*c*)

Fig. 7. Electronic images of the UAM-100 ultrafiltration membrane:
a – image of the membrane surface – its active layer; *b* – substrate surface, for this membrane – felted nylon;
c – image of the active cellulose acetate layer section of the membrane

in diameter as they approach the substrate [28]. It should be noted that the studied type of membranes is chemically and structurally heterogeneous. They consist of a highly porous substrate coated with a thin, dense film of another polymer.

A schematic representation of the ultrfiltration membrane is shown in Fig. 8.

Studies of the surface and drainage layers of ultrafiltration membranes by electron microscopy have shown that all membranes have an anisotropic structure – their structural parameters change along the membrane thickness. Therefore, for them, the pore space as a whole can be characterized only by the values of the total volumetric porosity and average pore radius (Fig. 9). To study these parameters, we used the method of nitrogen adsorption on an AUTOSORB-iQ-C sorbtometer (Quantachrome, USA).

Table 5 shows the results of studying the specific surface area and porous structure of the studied membranes.

The analysis of images obtained using scanning electron microscopy showed that the pores of UAM-50 and UAM-100 composite ultrafiltration membranes are within the range of up to 100 nm, while the average pore diameter of the membranes is 2.5÷40 nm. It is noted that the analysis of the obtained images of membranes and the parameters of their porous structure are practically comparable with the results obtained by other methods, for example, nitrogen adsorption.

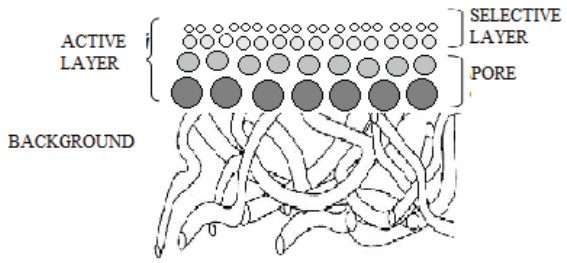

Fig. 8. Schematic representation of the ultrafiltration membrane [28]

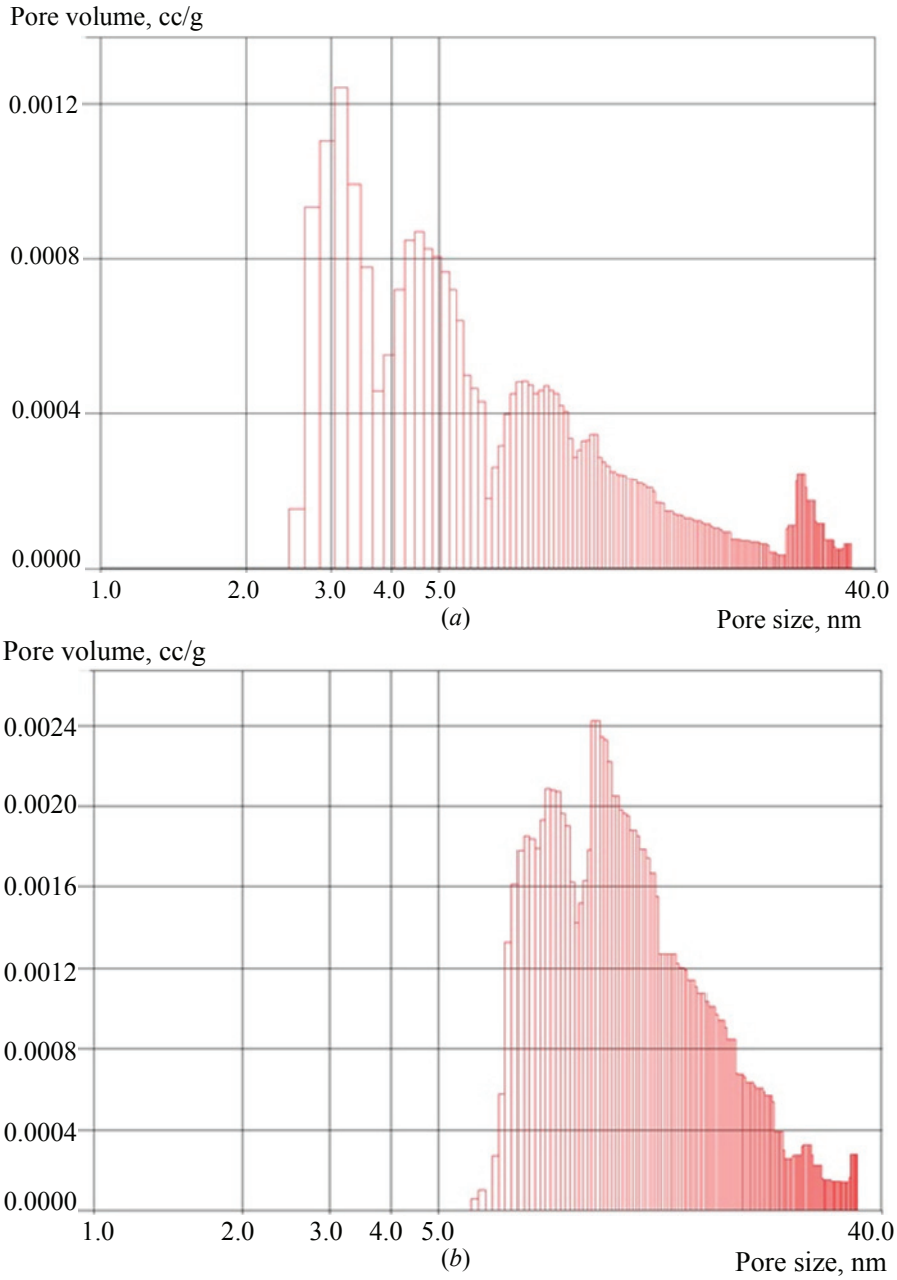

Fig. 9. Pore distribution histogram for UAM-50 (*a*) and UAM-100 (*b*) ultrafiltration membrane

Table 5. Characteristics of the UAM-50 and UAM-100 membranes

Investigated parameters	Membranes	
	UAM-50	UAM-100
Pore volume, $cm^3 \cdot g^{-1}$ (cc/g)	0.037	0.128
Surface area, $mL \cdot g^{-1}$	10.394	19.327
Lower confidence limit, nm	0.984	0.899
Installation error, %	6.829	3.103
Pore size, nm	3.169	10.681

3.3 Experimental studies of the hydrodynamic permeability of UAM-50, UAM-100 membranes

In experimental studies, the UAM-50 and UAM-100 industrial semi-permeable composite membranes were used, the main characteristics of which are given in Table 1 [32].

Before starting experimental studies, the membrane samples were visually checked for defects. Then they were immersed in the test solutions. Afterwards, a flat-chamber type separating ultrafiltration module was assembled. The membrane was fixed on a substrate (Whatman paper) so that the membrane did not have contact with metal surfaces,

the active layer to the solution to be separated. The shared module was attached to the laboratory setup described in [33]. The amount of collected permeate was determined every 30 minutes. At the end of the experiment, the pressure was released, the installation was turned off. The time was recorded with a stopwatch.

The experimental dependences of the hydrodynamic permeability for ultrafiltration membranes on the time of the separation process of a solution containing sodium lauryl sulfate was calculated by the formula (6):

$$\alpha = \frac{V}{F_m \tau P}, \quad (6)$$

where V is the volume of the collected permeate, m^3; F_m is the flat membrane working surface area, m^2; τ is the duration of experiment, s; P is the transmembrane pressure, MPa.

Fig. 10 shows the kinetic dependences of the hydrodynamic permeability on the time of the experiment.

As seen from Fig. 10, the hydrodynamic permeability during separation on an asymmetric membrane of cellulose acetate (UAM-50 (curve *1*), UAM-100 (curve *2*)) is variable over time.

When analyzing the dependences of the change in hydrodynamic permeability on time (τ), it was found that such dependences are well approximated by the sum of two exponential functions (Fig. 10) at ($R^2 = 0.976$)

$$J = y_0 + A_1 e^{-\tau k_1} + A_2 e^{-\tau k_2}, \quad (7)$$

where the values of the process rate constants – $k_1 = 1/\tau_1$, $k_2 = 1/\tau_2$ and the equation coefficients are given in Table 6.

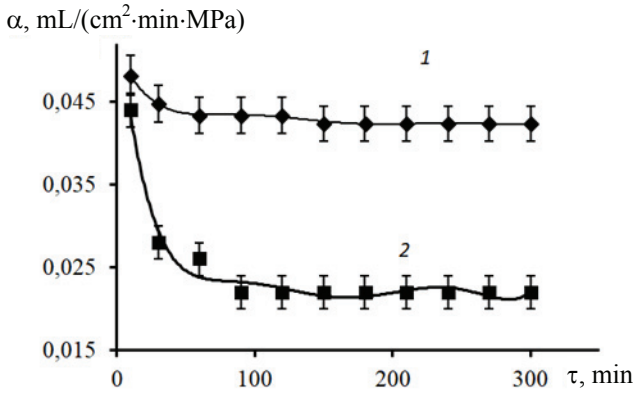

Fig. 10. The dependence of the hydrodynamic permeability on the time of the experiment for ultrafiltration membranes at a constant transmembrane pressure P = 1.0 MPa:
1 – UAM-50 series membrane;
2 – UAM-100 series membrane

Table 6. Design values of the process rate constants for UAM-50 and UAM-100 ultrafiltration composite membranes

Membrane parameters	y_0	A_1	A_2	τ_1	τ_2	R^2
UAM-50	0.042	0.0057	0.0035	13.05	60.85	0.975
UAM-100	0.022	0.0376	0.0151	7.87	33.11	0.977

Experimental studies of the hydrodynamic permeability of membranes during the separation of a solution containing sodium lauryl sulfate made it possible to determine that the kinetic curves of the response of the "membrane-solution" system under the action of transmembrane pressure can be conditionally divided into several stages. The first stage of the process was faster and lasted only a few minutes – 7.8 and 13.05 min, respectively. The hydrodynamic permeability decreased by ~ 27 % and 7 %, respectively. The observed effect was due to structural changes in the cellulose acetate layer under the action of mechanical stress (transmembrane pressure). The second stage was slower, lasting ~ 33 and 60 min, with a decrease in hydrodynamic permeability by 41 % and 11 %, respectively. Apparently, the decrease in permeability is associated with the process of structural rearrangement in the polymer substrate of the UAM-100 and UAM-50 membranes, respectively. At the same time, the dependence of the change in hydrodynamic permeability on the macroscopic parameters of the membranes, for example, such as pores, which undergo deformation and partial compression as a result of pressure, is noted. Earlier it was shown that the drainage layer of UV membranes UAM-50, UAM-100 is made of fabric-type and felted-type, respectively.

It is known that in the process of transmembrane separation, the process solution interacts with the active layer of the membrane, changes its structural properties, and the pressure compresses the active layer. As noted earlier in [34], the supramolecular structure of the cellulose acetate active layer of membranes is due to two types of hydrogen bonds – (OH···O), (CH···O=C) and the dipole-dipole interaction of carbonyl groups. Sorbed water breaks weak intermolecular bonds (CH···O) in the structure of cellulose acetate, which increases the polarity of carboxyl groups due to the induction effect. Therefore, strong hydrogen bonds with water molecules arise between the oxygen atoms of the polar groups of cellulose acetate, forming a

polymolecular layer of bound water. As a result, the pore size decreases and, accordingly, the hydrodynamic permeability of the permeate decreases.

4. Conclusions

Using the data on the study of the pore diameter and their distribution over the sample surface, an electron microscopy procedure was developed in conjunction with the use of the AutoCad 2018 computer-aided design system and Microsoft Excel 2010 tools, which made it possible to study the pore diameter distribution of UPM-K ultrafiltration membranes. As a result of the studies carried out, it was found that the size range of pore diameters on the surface of UPM-K membranes corresponds to the law of normal distribution, for which mathematical expressions have been obtained showing that for the UPM-K membrane sample the largest pore diameter is 70 nm, and the average pore diameter is 54 nm. For the UAM-50 and UAM-100 ultrafiltration membranes, it is noteworthy that their structure was asymmetric (active layer (dense) and porous substrate), and the pores had sizes from 2.5 to 40 nm and from 10 to 40 nm, respectively.

Experimental studies of the membranes hydrodynamic permeability allow to determine that the kinetic curves of the response of the "membrane-solution" system under the action of transmembrane pressure have several stages. The first stage of the process was 7.8 min and 13.05 min, and the hydrodynamic permeability decreased by ~ 27 % and 7%, respectively. The second stage was slower, lasting ~ 33 min and 60 min, with a decrease in hydrodynamic permeability by 41 % and 11 %, respectively. This was due to the process of structural rearrangement in the polymer substrate for the membranes.

5. Funding

This study did not receive external funding.

6. Conflict of interests

The authors declare no conflict of interest.

References

1. Ulbricht M. Advanced functional polymer membranes. *Polymer*. 2006;47(7):2217-2262. DOI:10.1016/j.polymer.2006.01.084

2. She Q, Wang R, Fane AG, Tang CY. Membrane fouling in osmotically driven membrane processes: A review. *Journal of Membrane Science*. 2016;(499):201-233. DOI:10.1016/j.memsci.2015.10.040

3. Jhaveri JH, Murthy ZVP. A comprehensive review on anti-fouling nanocomposite membranes for pressure driven membrane separation processes. *Desalination*. 2016;(379):137-154. DOI:10.1016/j.desal. 2015.11.009

4. Kotra-Konicka K, Kalbarczyk J, Gac JM. Modification of polypropylene membranes by ion implantation. *Chemical and Process Engineering*. 2016;37(3):331-339. DOI:10.1515/cpe-2016-0027

5. Ge Zh, He Zh. Effects of draw solutions and membrane conditions on electricity generation and water flux in osmotic microbial fuel cells. *Bioresource Technology*. 2012;(109):70-76. DOI:10.1016/j.biortech. 2012.01.044

6. Lazarev SI, Kovalev SV, Konovalov DN, Kovaleva OA. Analysis of kinetic characteristics of baromembrane and electrobaromembrane separation of ammonium nitrate solution. *Izvestiya vysshih uchebnyh zavedenij. Seriya: Himiya i himicheskaya tekhnologiya = ChemChemTech*. 2020;63(9):28-36. (In Russ.)

7. Kovalev SV, Lazarev SI, Kovaleva OA. A Study of the surface morphology of microfiltration membranes of the MFFK and MPS brands by atomic-force-and scanning-electron microscopy. *Journal of Surface Investigation: X-ray, Synchrotron and Neutron Techniques*. 2020;14(4):696-705. DOI:10.1134/ S1027451020040126

8. Lazarev SI, Golovin YM, Kovalev SV, Levin AA. Characteristics of thermal action on porous cellulose acetate composite material. *Journal of Engineering Physics and Thermophysics*. 2019;92(4):1050-1054. DOI:10.1007/s10891-019-02019-0.

9. Uglyanskaya VA, Chikin GA, Selemenev VF, Zavyalova TA. *Infrared spectroscopy of ion-exchange materials.* Voronezh: VSU; 1989. 208 p. (In Russ.)

10. Lazarev SI, Kovaleva OA, Popov R, Kovalev SV. Investigation of the process of ultrafiltration separation of technological solutions in the production of alcohol from molasses. *BestPrint: ion transport in organic and inorganic membranes: International conference: Conference Proceedings*. *Russian academy of sciences; section "membranes and membrane technologies" of D.I. Mendeleev; 2017, BESTPRINT, 23-27 May 2017, Russia,* Krasnodar: BestPrint; 2017. p. 212-214. (In Russ.)

11. Ryzhkin VYu, Lazarev SI, Kovalev SV, Konovalov DN, Mamontov AS, Lua P. Application of microfiltration, nanofiltration, and electronanofiltration processes to improve the efficiency of the solution separation scheme in biochemical production. *Publisher entrepreneur V. A. Chesnokov: topical issues of electrochemistry, environmental protection and*

corrosion: Materials of international conference dedicated to the memory of Professor, honored scientist of the Russian Federation V. I. Vigdorovich, 23-25 October 2019, Russia, Tambov: Publishing House V.A. Chesnokov; 2019. p. 447-450. (In Russ.)

12. Akram A, Stuckey D. Flux and performance improvement in a submerged anaerobic membrane bioreactor (SAMBR) using powdered activated carbon (PAC). *Process Biochemistry.* 2008;43(1):93-102. DOI:10.1016/j.procbio.2007.10.020

13. Pervov AG, Andrianov AP, Kondratiev VV, Spirov DV. Development of a computer program for the use of CSM (SAEHAN) nanofiltration membranes for the production of drinking and industrial water. *Membrany*. 2008;(1):9-18. (In Russ.)

14. Arkhangelsky E, Duek A, Gitis V. Maximal pore size in UF membranes. *Journal of Membrane Science.* 2012;394-395:89-97. DOI:10.1016/j.memsci. 2011.12.031

15. Khanukaeva DYu, Filippov AN, Bildyukevich AV. Investigation of ultrafiltration membranes using AFM: features of pore size distribution. *Membrany i membrannye tekhnologii = Petroleum Chemistry.* 2014;4(1):37-46. (In Russ.)

16. Yoon Y, Lueptow RM. Removal of organic contaminants by RO and NF membranes. *Journal of Membrane Science.* 2005;261(1-2):76-86. DOI: 10.1016/j.memsci.2005.03.038

17. Murthy ZVP, Choudhary A. Separation and estimation of nanofiltration membrane transport parameters for cerium and neodymium. *Rare Metals.* 2012;31(5):500-506. DOI: 10.1007/s12598-012-0547-y

18. Balandina AG, Hangildin RI, Ibragimov IG, Martyasheva VA. Development of membrane technologies and the possibility of their application for wastewater treatment of chemical and petrochemical enterprises. *Elektronnyj nauchnyj zhurnal "Neftegazovoe delo" = Oil and Gas Business.* 2015;(5):336-375. (In Russ.)

19. Vasin SI, Filippov AN. The permeability of complex porous media environments. *Kolloidnyj zhurnal = Colloid Journal.* 2009;71(1):32-46. (In Russ.)

20. Kumar S, Nandi BK, Guria C, Mandal A. Oil removal from produced water by ultrafiltration using polysulfone membrane. *Brazilian Journal of Chemical Engineering*. 2017;34(2):583-596. DOI:10.1590/ 0104-6632.20170342s20150500.

21. Karagunduz A, Dizge N. Investigation of membrane biofouling in cross-flow ultrafiltration of biological suspension. *Journal of Membrane Science & Technology.* 2013;3(1):1-5. DOI:10.4172/2155-9589. 1000120.

22. Kolzunova LG, Greben VP, Karpenko MA, Rodzik IG. Membrane separation methods and new membranes for these processes. *Vestnik Dal'nevostochnogo otdeleniya Rossijskoj akademii nauk = Vestnik of the Far East branch of the Russian academy of sciences.* 2009;2(144):13-17. (In Russ.)

23. Philippova TS, Filippov AN. Theoretical evaluation of the microfiltration membrane lifetime. *Petroleum Chemistry*. 2014;54(8):705-709. DOI:10.1134/S0965544114080064

24. Abdelrasoul A, Doan HD, Lohi A, Cheng Chil-Hung. Morphology control of polysulfone membranes in filtration processes: a critical review. *ChemBioEng Reviews.* 2015;2(1):22-43. DOI:10.1002/cben.201400030

25. Melnikova GB, Zhavnerko GK, Chizhik SA, Bildyukevich AV. Structure and mechanical properties of ultrafiltration membranes modified by Langmuir–Blodgett films. *Membrany i membrannye tekhnologii = Petroleum Chemistry.* 2016;6(2):144-151. (In Russ.)

26. *Membranes, filter elements, membrane technologies: catalog of CJSC STC "Vladipor".* 2007. 22 p.

27. Solonin IS. *Application of mathematical statistics in mechanical engineering technology.* Sverdlovsk: Central Ural Book Publishing House; 1966. 200 p. (In Russ.)

28. Khorokhorina IV, Lazarev SI, Golovin YuM, Arzamassev AA. Studies of the surface and drainage layers of ultrafiltration membranes by scanning electron microscopy. *Vestnik tekhnologicheskogo universiteta*. 2019;22(2):126-129. (In Russ.)

29. Lazarev SI, Golovin YuM, Shestakov KV, Kovalev SV. Features of X-ray diffractometric studies of the structural characteristics of polymer membranes. *Vestnik tekhnologicheskogo universiteta.* 2018;21(2):22-25. (In Russ.)

30. Kovaleva OA, Lazarev SI, Konovalov DN, Kovalev SV. Comparative study of methods of separation of technological solutions and waste water of electroplating industries. *Vestnik tekhnologicheskogo universiteta.*2018;21(5):58-63. (In Russ.)

31. Lazarev SI, Golovin YuM, Kovalev SV, Ryzhkin VYu. Method of automated determination of the morphology of the selectively permeable surface of polymer membranes OPMN-P and OFAM-K. *Zavodskaya laboratoriya. Diagnostika materialov = Industrial Laboratory. Diagnostics of Materials.* 2018;84(9):34-40. (In Russ.)

32. *Vladipor: membranes and filter elements.* Available from: http://www.vladipor.ru [Accessed 18 March 2019]. (In Russ.)

33. Lazarev SI, Gorbachev AS, Kuznetsov MA. Influence of pressure, temperature, and concentration on the reverse osmotic separation of an aqueous solution of sodium sulfonylate. *Izvestiya vysshih uchebnyh zavedenij. Seriya: Himiya i himicheskaya tekhnologiya = ChemChemTech*. 2005;48(4):126-129. (In Russ.)

34. Lazarev SI, Golovin YuM, Kovalev SV. Structural characteristics and state of water in the cellulose acetate membrane. *Theoretical Foundations of Chemical Engineering.* 2016;50(3):294-302. DOI:10.1134/S0040579516030076

Информация об авторах / Information about the authors

Лазарев Сергей Иванович, доктор технических наук, профессор, Тамбовский государственный технический университет (ФГБОУ ВО «ТГТУ»), Тамбов, Российская Федерация; ORCID 0000-0003-0746-5161; e-mail: mig@tstu.ru

Ковалева Ольга Александровна, доктор технических наук, доцент, Тамбовский государственный университет имени Г.Р. Державина, ФГБОУ ВО «ТГТУ», Тамбов, Российская Федерация; ORCID 0000-0003-0735-6205; e-mail: solomina-oa@yandex.ru

Хорохорина Ирина Владимировна, кандидат технических наук, доцент, ФГБОУ ВО «ТГТУ», Тамбов, Российская Федерация; ORCID 0000-0001-8722-3685; e-mail: kotelnikovirina@yandex.ru

Хромова Татьяна Александровна, аспирант, ФГБОУ ВО «ТГТУ», Тамбов, Российская Федерация; ORCID 0000-0002-8743-9918; e-mail: tatyanka.xromova96@mail.ru

Ковалев Сергей Владимирович, доктор технических наук, доцент, ФГБОУ ВО «ТГТУ», Тамбов, Российская Федерация; ORCID 0000-0002-5961-7561; e-mail: sseedd@mail.ru

Sergey I. Lazarev, D. Sc. (Engineering), Professor, Tambov State Technical University (TSTU), Tambov, Russian Federation; ORCID 0000-0003-0746-5161; e-mail: mig@tstu.ru

Olga A. Kovaleva, D. Sc. (Engineering), Associate Professor, Derzhavin Tambov State University, TSTU, Tambov, Russian Federation; ORCID 0000-0003-0735-6205; e-mail: solomina-oa@yandex.ru

Irina V. Khorokhorina, Cand. Sc. (Engineering), Associate Professor, TSTU, Tambov, Russian Federation; ORCID 0000-0001-8722-3685; e-mail: kotelnikovirina@yandex.ru

Tatyana A. Khromova, Postgraduate, TSTU, Tambov, Russian Federation; ORCID 0000-0002-8743-9918; e-mail: tatyanka.xromova96@mail.ru

Sergey V. Kovalev, D. Sc. (Engineering), Associate Professor, TSTU, Tambov, Russian Federation; ORCID 0000-0002-5961-7561; e-mail: sseedd@mail.ru

Received 10 December 2020; Accepted 17 February 2021; Published 21 April 2021